Reciprocal Interactions in the Turtle Hindlimb Enlargement Contribute to Scratch Rhythmogenesis

SCOTT N. CURRIE AND GREGORY G. GONSALVES
Department of Neuroscience, University of California, Riverside, California 92521

Currie, Scott N. and Gregory G. Gonsalves. Reciprocal interactions in the turtle hindlimb enlargement contribute to scratch rhythmogenesis. *J. Neurophysiol.* 81: 2977–2987, 1999. We examined interactions between the spinal networks that generate right and left rostral scratch motor patterns in turtle hindlimb motoneurons before and after transecting the spinal cord within the anterior hindlimb enlargement. Our results provide evidence that reciprocal inhibition between hip circuit modules can generate hip rhythmicity during the rostral scratch reflex. ''Module'' refers here to the group of coactive motoneurons and interneurons that controls either flexion or extension of the hip on one side and coordinates that activity with synergist and antagonist motor pools in the same limb and in the contralateral limb. The ''bilateral shared core'' hypothesis states that hip flexor and extensor (HF and HE) circuit modules interact via crossed and uncrossed spinal pathways: HF modules make reciprocal inhibitory connections with contralateral HF and ipsilateral HE modules and mutual excitatory connections with contralateral HE modules. It is currently unclear how much reciprocal inhibition between modules contributes to scratch rhythmogenesis. To address this issue, fictive scratch motor patterns were recorded bilaterally as electroneurograms from HF, HE, knee extensor (KE), and respiratory (d.D8) muscle nerves in immobilized animals. *D_3-end* (low-spinal) preparations had intact spinal cords posterior to a complete D_2–D_3 transection. Unilateral stimulation of rostral scratch in D_3-end turtles elicited rhythmic alternation between ipsilateral HF and HE bursts in most cycles; consecutive HF bursts were separated by complete silent (HF-OFF) periods. *D_3–D_9* and *D_3–D_8* preparations received a second spinal transection at the caudal end of segment D_9 or D_8, respectively, within the anterior hindlimb enlargement. This second transection disconnected most HE circuitry (located mainly in segments D_{10}–S_2 of the posterior enlargement) from the rostral scratch network and thereby reduced the HE-associated inhibition of HF circuitry. Unilateral stimulation of rostral scratch in most D_3–D_9 and D_3-D_8 preparations evoked rhythmic or weakly modulated ipsilateral HF discharge without HF-OFF periods between bursts and without ipsilateral HE activity in the majority of cycles. In contrast, bilateral stimulation in D_3–D_9 and D_3–D_8 preparations reconstructed the HF-OFF periods, increased HF rhythmicity (assessed by fast Fourier transform power spectra and autocorrelation analyses), and reestablished weak HE-phase motoneuron activity. We suggest that bilateral stimulation produced these effects by simultaneously activating reciprocally inhibitory hip modules on opposite sides (right and left HF) and the same side (HF and residual ipsilateral HE circuitry). Our data support the hypothesis that reciprocal inhibition can contribute to spinal rhythmogenesis during the scratch reflex.

INTRODUCTION

A low-spinal turtle that is immobilized by neuromuscular blockade responds to cutaneous stimulation of the lateral midbody by generating a fictive rostral scratch motor pattern in ipsilateral hindlimb motoneurons (Robertson et al. 1985). Rostral cutaneous sensory input enters the midbody spinal cord segments (D_3–D_6) and activates rhythmic motor output from the hindlimb enlargement (D_8–D_{10}, S_1–S_2: innervating hindlimb muscles) and prehindlimb-enlargement segments (D_6–D_7: innervating respiratory muscles). In D_3-end preparations (low spinal animals with a complete cord transection between segments D_2 and D_3), unilaterally evoked fictive rostral scratching is characterized by rhythmic alternation between ipsilateral hip flexor (HF) and hip extensor (HE) bursts and monoarticular knee extensor (KE) discharge during the late HF phase (Robertson et al. 1985). There is also weaker rhythmic motor output from contralateral hindlimb (Currie and Lee 1997; Stein et al. 1995, 1998) and preenlargement (Currie and Gonsalves 1997) muscle nerves that alternates with ipsilateral activity. Simultaneous bilateral stimulation in the right and left rostral receptive fields elicits bilateral rostral scratch motor patterns in which homologous nerve activity alternates on the right and left sides (Currie and Gonsalves 1997; Currie and Lee 1997; Stein et al. 1995, 1998). These results establish that there is an alternating phase relationship, probably involving reciprocal inhibition, between mirror-image hip circuitry (e.g., HF) on the right and left sides and between hip antagonist circuitry (HF and HE) on the same side during fictive rostral scratching. Recent experiments in our laboratory indicated that reciprocal inhibition could generate rhythmic activation of respiratory motoneurons in the prehindlimb-enlargement turtle spinal cord (Currie and Gonsalves 1997). In the present experiments, we assessed the ability of reciprocal inhibition between *hip* circuit modules to generate rhythmic motoneuron activity. According to the ''bilateral shared core'' model (Stein et al. 1995), HF and HE modules, comprising the core of the scratch rhythm generator, interact via crossed and uncrossed synaptic pathways: HF modules make reciprocal inhibitory connections with contralateral HF and ipsilateral HE modules and mutual excitatory connections with contralateral HE modules. These connections are supported by more recent studies (Currie 1997; Currie and Lee 1997; Stein et al. 1998). We disconnected as much HE circuitry as possible from the right and left rostral scratch networks by completely transecting the spinal cord at the caudal end of segment D_9 or D_8 in the anterior enlargement; this created D_3–D_9 and D_3–D_8 preparations, respectively. The cell bodies of HE motoneurons are distributed from segment D_9 to S_2 at the posterior end of the enlargement and are most concentrated in segments D_{10}–S_2 (Ruigrok and Crowe 1984). HF motoneurons are distributed more anteriorly, in segments D_8–D_9. Lesion experiments by Mortin and Stein (1989) suggested that at least some of the premotor circuitry for HF and

The costs of publication of this article were defrayed in part by the payment of page charges. The article must therefore be hereby marked ''*advertisement*'' in accordance with 18 U.S.C. Section 1734 solely to indicate this fact.

HE was located in the same segments as the motoneurons. Those authors created isolated D_8 and D_8–D_9 preparations by completely transecting the spinal cord at the anterior and posterior ends of those segments. Rhythmic HF motor discharge, lacking quiescent (HF-OFF) periods between bursts, still could be elicited in these animals by tactile stimulation within the pocket scratch receptive field. That result showed that sufficient interneuronal circuitry exists within the D_8 and D_9 segments to generate rhythmic discharge in HF motoneurons. Similar rhythmic HF discharge without HF-OFF periods also was exhibited by D_3–D_9 and D_3–D_8 preparations in that study, indicating that HE circuitry, mainly located posterior to D_9, was required for normal inhibition of HF motoneurons between bursts. Thus by cutting away the posterior enlargement in the present experiments, we removed a large fraction of HE circuitry from the rostral scratch network and greatly reduced the HE-associated inhibition of ipsilateral HF discharge. Our data show that during unilateral stimulation of rostral scratch, most D_3–D_9 and D_3–D_8 turtles displayed a low percentage of normal HF cycles with complete off periods between bursts, confirming the earlier work by Mortin and Stein (1989). In contrast, bilateral stimulation of rostral scratch produced vigorous, alternating discharge in right and left HF nerves with restored HF-OFF periods on both sides and greatly increased HF rhythmicity. Our experiments support the hypothesis that reciprocal inhibition in the anterior hindlimb enlargement can contribute to hindlimb rhythmogenesis during rostral scratch motor patterns. Portions of this work were published in an extended abstract (Currie and Gonsalves 1998).

METHODS

Red-eared slider turtles (n = 11), *Trachemys scripta elegans*, weighing 470–650 g, were placed in crushed ice for a minimum of 2 h before surgery to induce hypothermic anesthesia (Lennard and Stein 1977). Turtles were maintained partially immersed in crushed ice during all surgical procedures. The first surgical procedure was complete transection of the spinal cord just posterior to the forelimb enlargement, between spinal segments D_2 and D_3 (D_2 = the second postcervical segment) (Zangerl 1969).

Surgical procedures

Hindlimb muscle nerves were prepared bilaterally for electroneurographic (ENG) recording (see Fig. 1; nerves shown only on right side). The FT-KE and AM-KE nerves innervate triceps femoris pars femorotibialis and pars ambiens, respectively. VP-HP innervates puboischiofemoralis internus, pars anteroventralis, a hip flexor muscle. HR-KF innervates several bifunctional hip extensor-knee flexor muscles of the flexor tibialis group. Distal D8 (d.D8) innervates respiratory and pelvic muscles adjacent to the hindlimb. These nerves and the muscles they innervate have been described previously (Mortin and Stein 1989; Robertson et al. 1985). Motoneurons with axons in the d.D8 nerve exhibit two phases of activity during a scratch reflex: a HF-correlated burst and a HE-correlated burst (Currie and Lee 1996b; Mortin and Stein 1989). We used d. 8 as a monitor of HE activity in some D_3–D_8 preparations in which the entire HR-KF (HE) motor pool was removed by the D_8–D_9 cord transection. Hereafter in the text, FT-KE and AM-KE are referred to as KE nerves, VP-HP as the HF nerve, and HR-KF as the HE nerve. In four turtles, we prepared KE, HF, and HE nerves bilaterally (*experiments 1, 9, 10,* and *11*). In four other turtles, we prepared KE, HF, and d.D8 nerves bilaterally (*experiments 2–5*). In three turtles, we prepared only KE and HF nerves bilaterally (*experiments 6–8*). Each nerve was freed

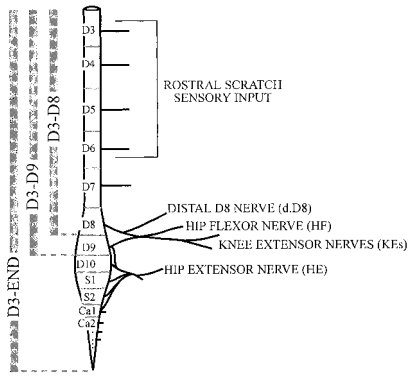

FIG. 1. Diagram of the turtle spinal cord, indicating sensory and motor components of the rostral scratch reflex (*right*) and the spinal segments included in D_3-end, D_3–D_9 and D_3–D_8 preparations (*left*). All preparations had a complete spinal transection just posterior to the forelimb enlargement between segments D_2 and D_3. D_3-end preparations had intact spinal cords posterior to the D_2–D_3 transection site. D_3–D_9 and D_3–D_8 preparations had a 2nd transection between segments D_9–D_{10} or D_8–D_9, respectively. Fictive rostral scratch motor patterns were elicited by electrical or mechanical stimulation of the shell in the right and/or left rostral scratch receptive field(s) and recorded bilaterally from hindlimb muscle nerves (shown on the *right* side only). Electroneurographic (ENG) recordings were obtained from a knee extensor (KE) nerve (either AM-KE or FT-KE), an hip flexor (HF) nerve (VP-HP), and either a hip extensor (HE) nerve (HR-KF) or the distal D8 nerve (d.D8), which exhibits HF- and HE-correlated motor bursts. See METHODS for a more detailed identification of peripheral nerves and a description of surgical procedures.

from surrounding tissues, tied with surgical thread near its muscle insertion, and then cut distal to the tie.

We exposed spinal cord segments D_8–D_{10} at the anterior side of the hindlimb enlargement by drilling a dorsal midline channel through the carapace and performing a dorsal laminectomy. The turtle hindlimb enlargement consists of three dorsal segments (D_8, D_9, D_{10}) and two sacral segments (S_1, S_2; Fig. 1). In five turtles (*experiments 1–5*), we covered the exposed cord with saline-soaked Gelfoam surgical sponge so that the spinal cord could be transected later at the caudal end of the D_8 (n = 4) or D_9 (n = 1) segment, during the experiment. In six turtles (*experiments 6–11*), we transected the cord during the initial dissection at the caudal end of D_8 (n = 2) or D_9 (n = 4), while the turtle was still on ice. Transections were performed under a dissection microscope with fine iridectomy scissors. The completeness of transections was confirmed visually by lifting one of the cut ends of the spinal cord upward with forceps, viewing the cord in cross-section, and then replacing it in the spinal canal.

ENG recordings and data storage

After surgery was complete, preparations were allowed to warm up to room temperature and then were immobilized with an intramuscular injection of gallamine triethiodide (8 mg/kg body wt; Sigma, St. Louis, MO). The trachea was intubated and artificial respiration used throughout the experiment. The skin was kept moist with turtle saline. Three separate rings of warm dental wax were formed around the holes in the dorsal carapace over the right and left hindlimb nerves and the exposed spinal cord, allowed to cool and harden, and glued in place with cyanoacrylate adhesive. The dissected hindlimb nerves were arrayed for recording by securing their attached threads to the rim of the wax well. The wells surrounding hindlimb nerves were filled with mineral oil; the well surrounding the exposed spinal cord was filled with turtle saline. Bipolar hook electrodes (100 μm diam silver) were used to record from the nerves, electrically insulated by the mineral oil. ENG signals were amplified and filtered (band-pass 100 Hz to 1 kHz), digitized by a PCM video adapter (Vetter; Rebersburg, PA) and stored along with a voice channel and stimulus marker on videotape (band-pass DC, 3.5 kHz). Hard copies of all recordings

TABLE 1. *Bilateral stimulation of rostral scratch reconstructed normal* HF-OFF *periods in D_3–D_9 and D_3–D_8 preparations*

			Unilateral Stimulation		Bilateral Stimulation	
Experiment	Preparation	Stimulation	Number of Episodes	Average Percent of Cycles per Episode with Normal HF-OFF Periods	Number of Episodes	Average Percent of Cycles per Episode with Normal HF-OFF Periods
1 (E)	D_3–D_9	Right	4	0.0 (0.0)	4	100.0 (0.0)*
		Left	4	20.8 (25.0)	4	95.8 (8.4)†
3 (M)	D_3–D_8	Right	6	43.9 (15.8)	6	85.3 (11.2)*
		Left	6	55.0 (24.5)	6	88.1 (7.1)*
6 (E)	D_3–D_9	Right	5	0.0 (0.0)	5	70.0 (18.2)*
		Left	5	0.0 (0.0)	5	76.7 (13.7)*
7 (M)	D_3–D_8	Right	10	0.0 (0.0)	10	79.7 (10.9)‡
		Left	10	3.3 (7.0)	10	72.2 (10.3)‡
8 (M)	D_3–D_9	Right	3	0.0 (0.0)	3	66.4 (3.8)†
		Left	3	0.0 (0.0)	3	48.6 (7.3)†
9 (M)	D_3–D_9	Right	12	0.9 (3.2)	12	74.8 (8.2)‡
		Left	12	15.6 (18.8)	12	87.3 (6.4)‡
10 (M)	D_3–D_9	Right	10	0.0 (0.0)	10	61.4 (12.2)‡
		Left	10	0.0 (0.0)	10	67.8 (14.3)‡
11 (E)	D_3–D_8	Right	10	84.4 (8.6)	10	92.9 (6.1)*
		Left	10	84.7 (12.5)	10	98.8 (3.9)*

Comparison of hip flexor (HF) electroneurographic cycles during unilateral and bilateral stimulation of rostral scratch receptive field(s). Either electrical (E) or mechanical (M) stimulation was used. Average percentages and their SDs (in parentheses) were calculated from percentages of cycles per episode showing complete HF-OFF periods (see *Data analysis*). Statistical significance within each experiment (bilateral stim. vs. unilateral stim.) was determined by the one-tailed Mann-Whitney *U* test (Siegel 1956). * $P < 0.01$. † $P < 0.04$. ‡ $P < 0.0001$.

from each experiment were printed with an eight-channel thermal-array recorder (Astro-Med; West Warwick, RI). Selected sequences also were redigitized off-line at 2 kHz per channel on a PC computer using a Digidata 1200A A-D converter with Axotape 2.0 software (Axon Instruments; Foster City, CA), formatted with Datapac II (Run Technologies; Laguna Hills, CA) and Coreldraw (Corel; Ottawa, Canada) software, and plotted on a laser printer.

Stimulation

We used either mechanical or electrical stimulation of the shell to evoke fictive rostral scratch reflexes. Scratch episodes always were separated by rest periods of ≥2 min. Mechanical stimulation was applied by gently rubbing a site on the shell with a fire-polished glass probe. In some cases, the probe was mounted on a hand-held force transducer (Grass Instruments-Astro-Med) to record the force and timing of the stimulus. Rubs with the glass probe were applied with a force of 0.2–1.4 N and lasted 15–20 s. Electrical stimulation was applied either unilaterally or bilaterally to sites in the rostral scratch receptive field via pin electrodes inserted into the shell epidermis 2–3 mm apart (Currie and Stein 1990). Pulses of 10- to 20-V amplitude and 1-ms duration were delivered in 50-pulse trains with an interpulse interval of 320 ms. For experiments in which bilateral electrical stimulation was applied, pin electrodes were inserted into mirror-image sites (SP2 or SP2.5) (see Mortin and Stein 1990) in the right and left rostral scratch receptive fields; during bilateral stimulation, identical trains of synchronized pulses were delivered to both sides. Unilateral and bilateral stimulus trains were applied in the following sequence: right, left, bilateral, bilateral, right, left (Stein et al. 1995).

Data analysis

PERCENTAGE OF SCRATCH CYCLES WITH NORMAL HF-OFF PERIODS. To determine the average percentage of rostral (Table 1) or pocket (RESULTS) scratch cycles per episode with normal HF-OFF periods, we examined thermal-array printouts of scratch ENGs. The total number of complete scratch cycles that occurred during stimulation was determined for each episode. Within an episode, we counted the number of ''normal'' cycles in which the HF ENG burst was followed by a period of complete quiescence (an HF-OFF period; e.g., Fig. 2, *A1* and *C1*) and the number of cycles in which the HF burst was followed by a period of reduced ENG amplitude but not complete quiescence (no HF-OFF period; e.g., Fig. 3, *A1* and *C1*). We defined an HF burst as a period of increased HF ENG amplitude that was accompanied by coactive discharge in the ipsilateral KE (AM-KE or FT-KE for rostral scratch episodes; AM-KE for pocket scratch episodes) or the contralateral HE nerve. In three D_3–D_8 preparations (*experiments 2, 4,* and *5*), clear HF bursts could not be reliably identified during unilateral stimulation of rostral scratch (e.g., Fig. 3*A2*); these experiments were excluded from the analysis in Table 1.

RECTIFIED-SMOOTHED ENG RECORDINGS. Rectified-smoothed ENG data (shown in Figs. 4, *A* and *B*, and 5 and used in time series analyses) were prepared by digitizing HF nerve recordings (100 Hz to 1 kHz bandwidth) off-line at 2 kHz per channel; digitized files then were full-wave rectified, rebinned at 100 Hz with a 100-point nonmoving average (50-ms binwidth), and smoothed with an even-weighted 10-point moving average (100-ms binwidth), using Datapac II software.

TIME SERIES ANALYSES. Time series analyses were used to examine rectified-smoothed HF nerve recordings for periodic trends in burst amplitude (autocorrelation, power spectra) and to identify relations between HF bursts on the right and left sides and any time delays between those bursts (cross-correlation). For autocorrelations, recordings from the left HF nerve, each consisting of 1,024 data points (10.23 s at a 100-Hz sampling rate) and beginning 3 s after stimulus-onset, were obtained from four consecutive rostral scratch episodes evoked by left stimulation (Fig. 4*C*) and four consecutive episodes evoked by bilateral stimulation (Fig. 4*D*) in *experiment 2*. Left-stimulation data were concatenated end to end into a single 4,096-point ASCII file; bilateral-stimulation data were concatenated into a second ASCII file. Both files then were imported into the Systat 7.0 software package (SPSS; Chicago, IL) for analysis. Cross-correlation (Fig. 5*B*) was performed on the same four bilateral-stimulation episodes used in Fig. 4D by importing both left and right HF recordings (1,024 points per channel), as a single ASCII file, into the Systat program. Plots show the correlation of the time series variable (HF voltage) with itself (autocorrelation) or with the contralateral nerve series (cross-correlation), negatively shifted by a number of time lags = 1, 2, 3, etc. The maximum number of lags in correlation plots was 500, lag duration was 10 ms.

Power spectrum analyses were performed on rectified-smoothed left HF nerve signals with a fast Fourier transform (FFT) program in

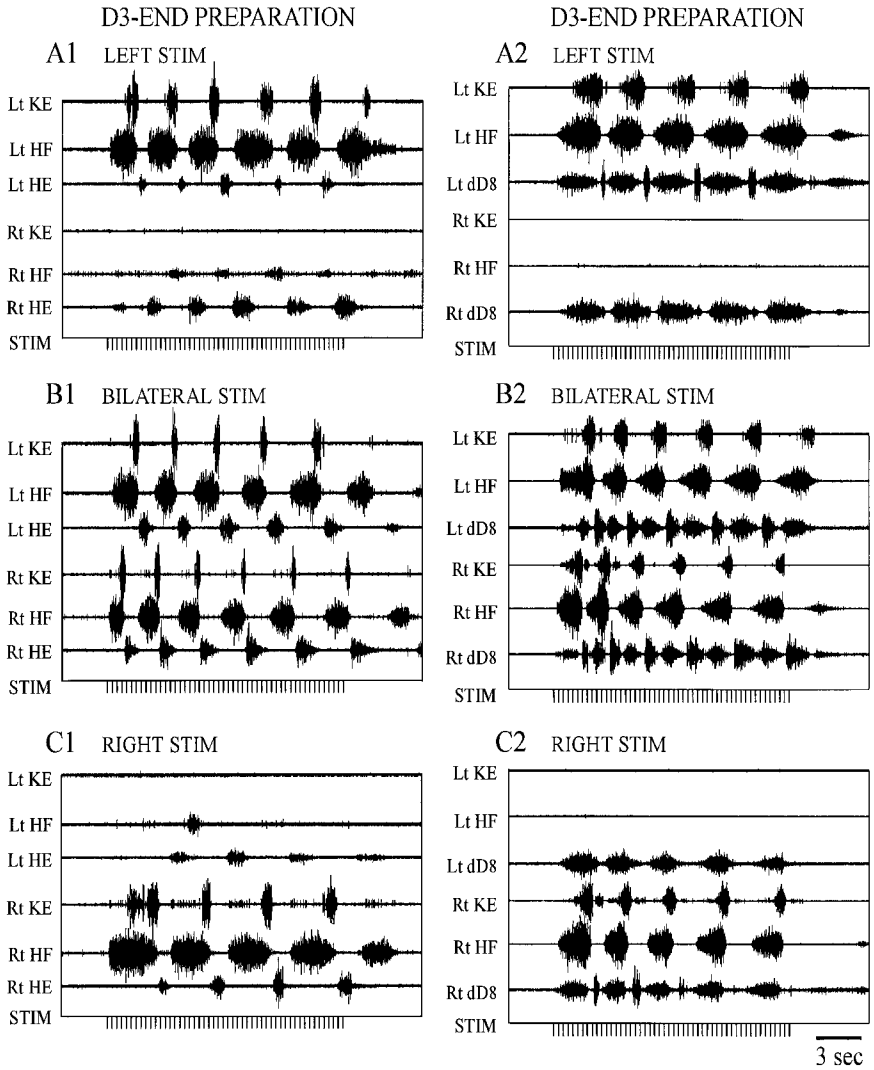

FIG. 2. Normal fictive rostral scratching evoked by unilateral and bilateral stimulation of rostral receptive fields in 2 different D_3-end preparations. *A1–C1*: bilateral recordings from KE (FT-KE), HF, and HE muscle nerves in *experiment 1*. *A2–C2*: bilateral recordings from KE (FT-KE), HF, and d.D8 nerves in *experiment 2;* note that the d.D8 nerve exhibited both HF- and HE-correlated bursts during each scratch cycle. Responses were elicited by trains of 50 electrical stimulus pulses (10-V, 1-ms pulses, 320-ms interpulse intervals) applied to the SP2.5 sites in the rostral receptive fields on the left side (*A, 1* and *2*), on both sides (*B, 1* and *2*), and on the right side (*C, 1* and *2*). During bilateral stimulation (*B, 1* and *2*), agonist nerves (e.g., HF) exhibited alternating activity on the right and left sides.

the Datapac II software package. In Fig. 4, *E* and *F*, the average power spectra were calculated for four consecutive rostral scratch episodes evoked by left stimulation (Fig. 4*E*) and four consecutive episodes evoked by bilateral stimulation (Fig. 4*F*) in *experiment 2*, using the same 1,024-point data sequences that were analyzed by autocorrelation in Fig. 4, *C* and *D*. The DC offset was removed from each data sequence by calculating the mean voltage for the entire sequence, then subtracting that value from each data point. Removing DC offset greatly reduced low-frequency components (0.0–0.1 Hz) in the power spectra, which when present, tended to mask nearby higher-frequency peaks. In Fig. 6, we calculated the average total power within the 0.29- to 0.49-Hz bandwidth for 16 scratch episodes (4 episodes each from 4 different experiments) in each of the following categories: left stimulation in D_3–D_8 preparations, bilateral stimulation in D_3–D_8 preparations, left stimulation in D_3–D_9 preparations, bilateral stimulation in D_3–D_9 preparations. The D_3–D_8 preparations chosen for analysis were *experiments 2, 4, 5,* and *7;* two other experiments (*3* and *11*) were excluded because they exhibited normal HF-OFF periods in >50% of rostral scratch cycles during left stimulation (see Table 1). The D_3–D_9 preparations were *experiments 1, 6, 9,* and *10;* one other experiment (*8*) was excluded because of an insufficient number of scratch episodes. We calculated total power as

$$\sum_{i=1}^{i=3} P_i$$

where P_i = the power coefficient of frequency component *i*, and 3 = the number of frequency components within the specified bandwidth (0.29, 0.39, 0.49 Hz).

RESULTS

Unilateral and bilateral stimulation of rostral scratch in D_3-end preparations

UNILATERAL STIMULATION. Bilateral ENG recordings were obtained from hindlimb (HF, HE, KE) and respiratory (d.D8) muscle nerves during fictive rostral scratch motor patterns in five D_3-end preparations that had intact spinal cords posterior to a D_2–D_3 transection site (Fig. 1). Fictive rostral scratching was elicited by mechanical or electrical stimulation (see METHODS) of the shell-surface within the rostral receptive field, located on the lateral ''shell-bridge,'' anterior to the hindlimb (Mortin and Stein 1990; Mortin et al. 1985). In one D_3-end preparation, we recorded from KE, HF, and HE nerves bilaterally (Fig. 2, *A1–C1*). During unilateral stimulation in the rostral receptive field, this turtle exhibited normal rhythmic alternation between HF and HE bursts ipsilateral to the stimulus and KE discharge during the late HF phase of each scratch cycle (Fig. 2, *A1* and *C1*) (see also Robertson et al. 1985). There was also weak rhythmic discharge in contralateral HE

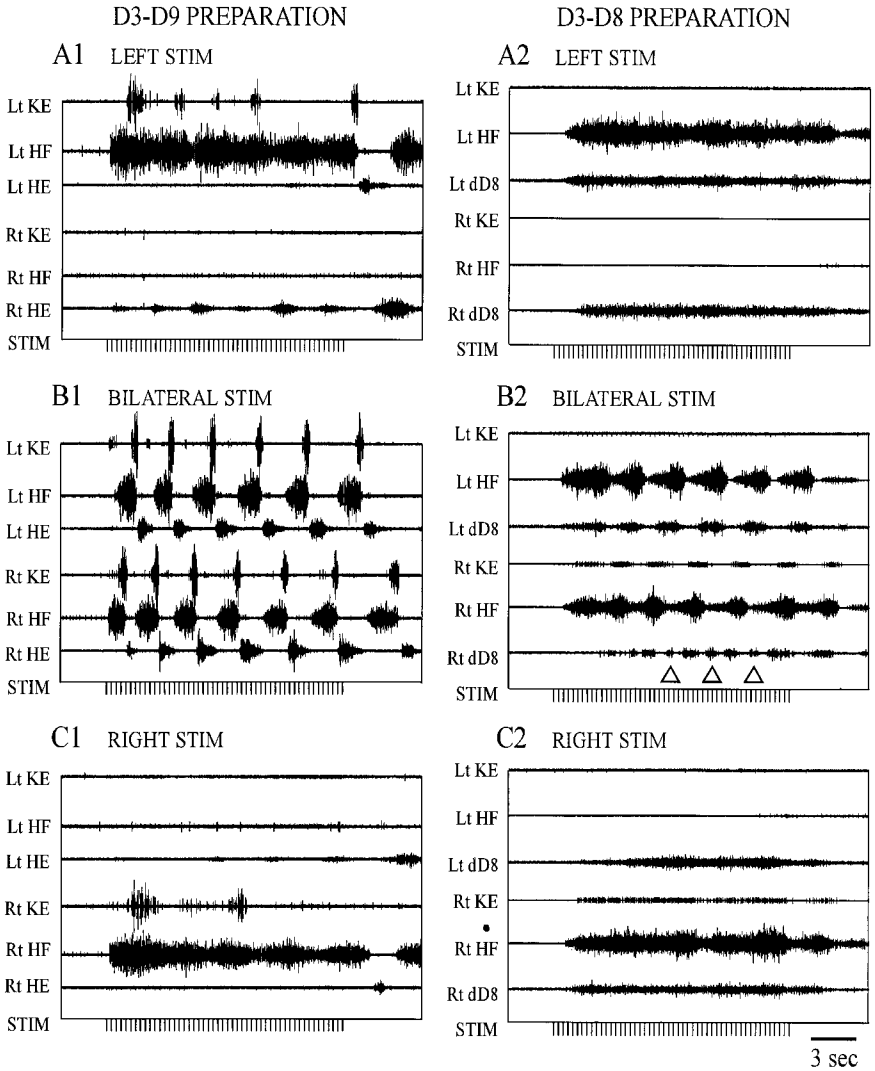

FIG. 3. Motor responses evoked by unilateral and bilateral stimulation of rostral receptive fields in a D_3–D_9 (*A1–C1*) and a D_3–D_8 (*A2–C2*) preparation. Same experiments and stimulus parameters as in Fig. 2. *A1–C1*: bilateral recordings from KE, HF, and HE nerves in *experiment 1* after spinal transection at the D_9–D_{10} border. *A2–C2*: bilateral recordings from KE, HF, and d.D8 nerves in *experiment 2* after spinal transection at the D_8–D_9 border. △, timing of HE-phase bursts in the right d.D8 nerve.

(Fig. 2, *A1* and *C1*) and HF (Fig. 2*A1*) nerves that was out-of-phase with ipsilateral activity (see also Currie and Lee 1997; Stein et al. 1995). In four other D_3-end preparations, we recorded from KE, HF, and d.D8 nerves bilaterally (e.g., Fig. 2, *A2–C2*), using d.D8 as a monitor of the HE phase of the scratch. Motoneurons with axons in the d.D8 nerve innervate respiratory muscle and exhibit two phases of activity during a scratch reflex: an HF-correlated burst and an HE-correlated burst (Currie and Lee 1996b; Mortin and Stein 1989). Among all D_3-end preparations, the average percentage of rostral scratch cycles per episode with normal HF-off periods was 86.6 ± 18.6% (62 episodes in 5 turtles) during unilateral stimulation. This is very close to the percentage of normal cycles observed during unilateral stimulation in previous work with D_3-end preparations (84.1%) (see Stein et al. 1998).

BILATERAL STIMULATION. Simultaneous stimulation of mirror-image sites in the right and left rostral receptive fields evoked bilateral rostral scratching in which the activity of homologous nerves (e.g., HF) alternated on the right and left sides (Fig. 2*B*, *1* and *2*) (see also Currie and Lee 1997; Stein et al. 1995, 1998). We observed right-left alternation of HF discharge during bilateral rostral scratching in all five D_3-end preparations in this study. We include these examples of normal unilateral and bilateral rostral scratching in the present paper so that direct comparisons can be made with the responses of D_3–D_9 and D_3–D_8 preparations, in which most HE circuitry was disconnected (see Fig. 3, following text).

Unilateral and bilateral stimulation of rostral scratch in D_3–D_9 and D_3–D_8 preparations

The D_3–D_9 and D_3–D_8 preparations in this study were created by a second spinal transection at the caudal end of the D_9 or D_8 segment, respectively, within the anterior hindlimb enlargement (Fig. 1). The somata of most HE motoneurons reside posterior to these transections in segments D_{10}–S_2, whereas HF motoneurons are distributed in segments D_8–D_9 (Ruigrok and Crowe 1984). Spinal transection experiments performed by Mortin and Stein (1989) indicated that some of the interneuronal circuitry associated with the HF and HE modules was located in the same segments as their respective motoneurons. Thus it is likely that our transections in the anterior enlargement disconnected most HE motoneurons and some associated premotor circuitry from the right and left rostral scratch networks. In five turtles, we transected at the caudal end of D_9 ($n = 1$) or D_8 ($n = 4$) after first recording D_3-end responses (see preceding text). In six other turtles, we transected the cord at the caudal end of D_9 ($n = 4$) or D_8 ($n = 2$) during the initial

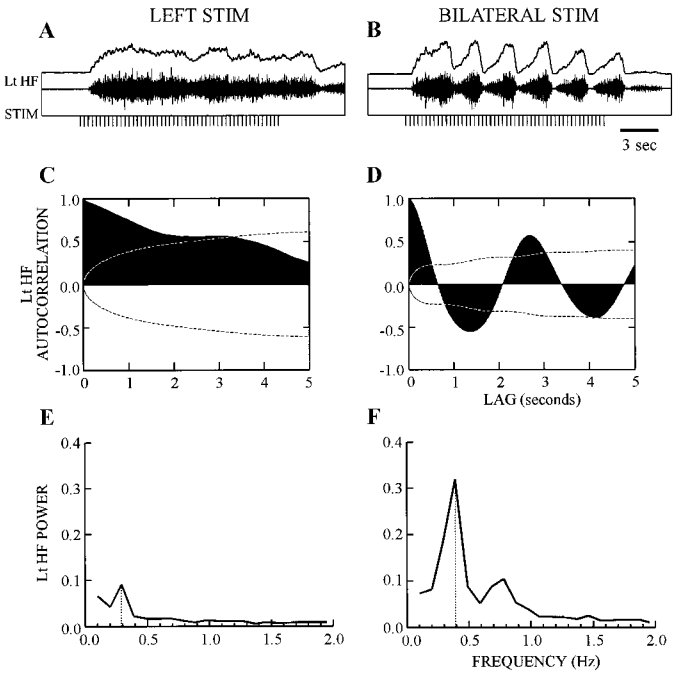

FIG. 4. Time-series analysis of periodicity in left HF motor output during left (*A*, *C*, and *E*) and bilateral (*B*, *D*, and *F*) stimulation of rostral scratch receptive fields. A, B, Raw (*middle traces*) and rectified-smoothed (*top*) ENG recordings from the left (Lt) HF nerve in a D_3–D_8 preparation. Same recordings shown in Fig. 3, *A2* and *B2*. Rectified-smoothed recordings (see METHODS) were used for all time-series analyses. *C* and *D*: autocorrelograms of rectified-smoothed recordings from the left HF nerve during 4 consecutive scratch episodes evoked by left stimulation (*C*) and 4 consecutive episodes evoked by bilateral (*D*) stimulation. Autocorrelograms are shown with means ± 2 SE (- - -). Bilaterally evoked responses exhibited a strong periodicity with alternation between positive and negative correlations; the cycle period (in *D;* measured from lag = 0 s to next positive peak) was 2.67 s. *E* and *F*: average fast Fourier transform (FFT) power spectra for the same scratch episodes used in *C* and *D*, respectively. Peak frequencies in *E* and *F* are indicated by vertical gray lines. During left stimulation (*E*), the peak power coefficient (0.09) occurred at a frequency of 0.29 Hz. During bilateral stimulation (*F*), the peak power coefficient (0.32) occurred at a frequency of 0.39 Hz, very close to the frequency (0.37 Hz) calculated from the autocorrelogram period in *D*. Secondary peak in *F*, to the right of the maximum, was a harmonic artifact.

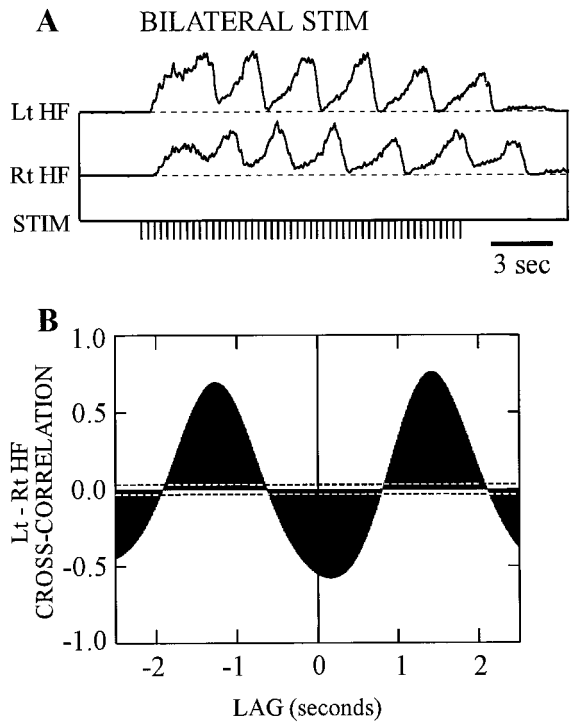

FIG. 5. Left and right HF bursts alternated in a D_3–D_8 preparation during bilateral stimulation of rostral scratch. *A*: rectified-smoothed ENG recordings from the left and right HF nerves in *experiment 2;* same scratch episode as shown in Figs. 3*B2* and 4*B*. *B*: cross-correlation of left and right HF bursts in same 4 consecutive bilateral scratch episodes analyzed in Fig. 4, *D* and *F*. Plot shows a near-maximum, highly significant negative correlation at lag = 0 s, indicating that left and right HF activity was close to 180° out of phase. Cycle period (2.67 s, measured between positive peaks) was identical to that of the autocorrelation in Fig. 4*D*. Cross-correlograms are shown with means ± 2 SE (- - -).

dissection, without recording D_3-end responses. All preparations were allowed ≥20 min to recover from cord transection before recording scratch responses. Turtles did not exhibit significant spinal shock because shell stimulation evoked robust fictive scratching within a few minutes after spinal transection (see also Mortin and Stein 1989). No significant change was noted in the rhythmicity or percentage of HF-OFF periods when comparing scratch responses 20–30 min after transection with responses obtained >12 h after transection (data not shown).

Because our transections in the enlargement removed most or all HE motoneurons in the majority of preparations, we did not always monitor HE motor output (see *Surgical procedures*). We focused instead on HF activity during unilateral and bilateral scratching because a large fraction of the HF motor pool and associated premotor circuitry is located within the D_8 segment (Mortin and Stein 1989; Ruigrok and Crowe 1984) and so, remained connected to the rostral scratch network in all D_3–D_9 and D_3–D_8 preparations. Some of our unilaterally evoked rostral scratch episodes (e.g., Fig. 3, *A1* and *C1*) contained cycles that could be described as ''HE deletions.'' HE deletions were defined in previous work as rostral scratch cycles that exhibit consecutive HF bursts without clear quiescent (HF-OFF) periods separating them and without corresponding HE bursts; to define these as rostral scratch cycles, the monoarticular knee extensor FT-KE also must be active during the latter part of each HF burst (Stein et al. 1995). In

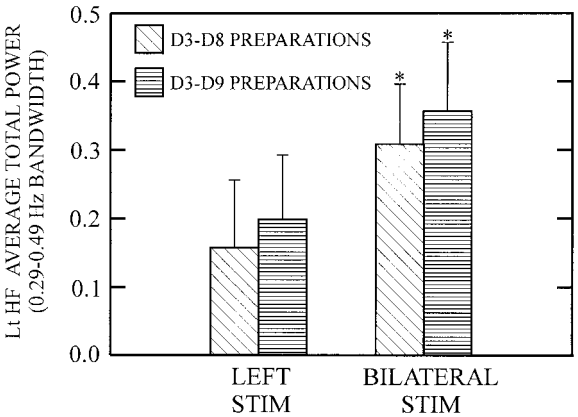

FIG. 6. Average total power calculated from FFT analysis of rectified-smoothed Lt HF recordings for the 0.29- to 0.49-Hz bandwidth, comparing episodes evoked by left and bilateral stimulation (see *Data analysis*). Each average was calculated for a total of 16 scratch episodes (4 episodes each from 4 different experiments). Bilateral stimulation produced a highly significant increase in the average integrated power within this frequency band for D_3–D_8 and D_3–D_9 preparations. Error bars indicate standard deviation values for the average power. Statistical significance within the D_3–D_8 and D_3–D_9 groups (bilateral stim. vs. left stim) was determined by the 1-tailed Mann-Whitney *U* test (Siegel 1956). * $P < 0.001$.

many of our D_3–D_9 and D_3–D_8 responses, HE activity was not recorded (e.g., Fig. 3, *A2–C2*), and the FT-KE nerve was often inactive during some cycles (e.g., latter part of Fig. 3*C1*) or during the entire scratch episode (Fig. 3, *A2–C2*). It was not possible to define such cycles as HE deletions, therefore we avoided that terminology. We refer instead to HF cycles with or without HF-OFF periods (see Table 1).

PERCENTAGE OF CYCLES WITH HF-OFF PERIODS DURING UNILATERAL AND BILATERAL STIMULATION. The D_3–D_9 preparation in Fig. 3, *A1–C1*, displayed strikingly different motor output within a given hindlimb in response to unilateral and bilateral stimulation of rostral scratch receptive fields. Unilaterally evoked responses did not exhibit normal alternation between HF and HE bursts during the period of stimulation (Fig. 3, *A1* and *C1*). Instead, these episodes displayed continuous, rhythmically modulated output from the ipsilateral HF nerve and weak KE discharge near the end of some, but not all HF bursts; there were no quiescent (HF-OFF) periods between HF bursts and no associated ipsilateral HE discharge during the period of stimulation. It is interesting, however, that both of the unilaterally evoked responses displayed a cycle of normal HF-HE alternation, with a complete HF-OFF period, after the end of the stimulus train. Such ''HE afterdischarges'' were very common during unilaterally evoked rostral scratch episodes in all three D_3–D_9 preparations in which we recorded from KE, HF, and HE nerves; we also observed the HF-OFF period after stimulus-offset in two other D_3–D_9 preparations where we recorded only KE and HF nerves. In contrast to unilaterally elicited responses, bilateral stimulation of rostral receptive fields reconstructed normal rostral scratch cycles with complete HF-OFF periods, near-normal HE burst-amplitudes, and strong KE discharge during the period of stimulation (Fig. 3*B1*). This result is consistent with the hypothesis of Stein et al. (1995; their Fig. 9) that HF modules make reciprocal inhibitory connections with contralateral HF and ipsilateral HE circuitry and mutual excitatory connections with contralateral HE circuitry.

The column labeled ''Unilateral Stimulation'' in Table 1 describes the average percentage of rostral scratch cycles per episode that displayed normal HF-OFF periods during unilateral stimulation of the rostral receptive field. Six D_3–D_8 and five D_3–D_9 preparations were tested; out of these 11 experiments, three D_3–D_8 preparations (*experiments 2, 4,* and *5*) were excluded from analysis in Table 1 because we were unable to reliably identify individual motor bursts in ipsilateral hindlimb nerves (see following text). The remaining eight preparations exhibited clear HF bursting during unilateral stimulation; of these, the majority ($n = 6$) displayed a very low percentage of cycles with normal HF-OFF periods (0.0–20.8%). Two other experiments, both D_3–D_8 preparations (*experiments 3* and *11*), were atypical in displaying a high percentage of cycles with normal HF-OFF periods during unilateral stimulation. The column labeled ''Bilateral Stimulation'' in Table 1 presents the average percentage of cycles per episode that exhibited normal HF-OFF periods during bilateral stimulation, ranging from 48.6 to 100.0%; all eight preparations displayed a significant increase in the percentage of cycles with HF-OFF periods compared with unilateral stimulation.

COMPARISON OF HF RHYTHMICITY DURING UNILATERAL AND BILATERAL STIMULATION. In three of six D_3–D_8 turtles, unilateral stimulation of the rostral receptive field elicited only irregular, modulated discharge in the ipsilateral HF and d.D8 nerves; individual HF bursts could not be reliably identified during unilateral stimulation (e.g., Fig. 3*A2*). In these preparations, bilateral stimulation did not reestablish complete HF-OFF periods but did significantly increase HF ''rhythmicity'' (regular periodic modulations of ENG amplitude) compared with unilateral stimulation (e.g., Fig. 3*B2*). During bilaterally evoked responses, distinct bursting appeared de novo in the right and left HF recordings and alternated from side to side. Small HE phase bursts also were displayed by the right d.D8 respiratory nerve during the low points between right HF bursts (Fig. 3*B2*, △), indicating that some HE-associated circuitry was present within the D_3–D_8 spinal cord and could be activated during bilateral stimulation. The increase in HF rhythmicity that occurred during bilateral stimulation was even more apparent in rectified-smoothed ENG recordings (Fig. 4, *A* and *B*) and in autocorrelation plots (Fig. 4, *C* and *D*). Spectral analyses were also performed using an FFT algorithm (Fig. 4, *E* and *F*); these showed that during bilateral stimulation, a large power peak developed at a frequency of 0.39 Hz, corresponding to an average cycle period of 2.56 s. This value is in good agreement with the average cycle period measured between the first and second positive peaks in the autocorrelogram (2.67 s; Fig. 4*D*).

Figure 5 shows a cross-correlogram of rectified-smoothed left and right HF recordings during bilateral stimulation. Note that it is also highly periodic and shows a near-maximal negative correlation at lag 0, indicating that left and right HF bursts were tightly coupled and out of phase. The cycle period measured from peak to peak in this cross-correlogram was 2.67 s, the same as that obtained from the autocorrelogram in Fig. 4*D*.

Pooled FFT data showed that bilateral stimulation increased the average total power (see *Data analysis*) within the 0.29–0.49 Hz bandwidth for D_3–D_8 ($n = 4$) and D_3–D_9 ($n = 4$) preparations relative to unilateral stimulation (Fig. 6). This increase was significant for both groups at $P < 0.001$, using the one-tailed Mann-Whitney *U* test (Siegel 1956).

Unilateral stimulation of pocket scratch in D_3–D_9 and D_3–D_8 preparations

Fictive pocket scratching was elicited by mechanical stimulation of the shell-skin border within the ventral pocket receptive field, located ventral and anterior to the thigh within the ''hindlimb pocket'' region (Mortin and Stein 1990; Mortin et al. 1985). Normal rostral and pocket scratch motor patterns in D_3-end preparations exhibit different knee extensor (AM-KE and FT-KE) timing within the HF-HE activity cycle (Robertson et al. 1985). In the rostral scratch, both FT-KE and AM-KE bursts begin and end during the HF phase. During the pocket scratch, FT-KE bursts begin and end during the HE (HF-OFF) phase, whereas AM-KE bursts begin during the HF phase and cease during the HE phase. In the present experiments, we compared HF activity during fictive pocket and rostral scratch responses in D_3–D_9 and D_3–D_8 turtles. Unilaterally evoked pocket scratch responses displayed a high percentage of normal HF cycles with clear HF-OFF periods in D_3–D_9 and D_3–D_8 preparations, in contrast to the near-zero percentage observed during unilaterally evoked rostral scratching in the same preparations. Figure 7*A* shows a rostral scratch episode from a D_3–D_9 preparation in which there was rhythmic HF discharge with no HF-OFF periods between most bursts. Figure 7*B* shows a pocket scratch episode from this same animal in which

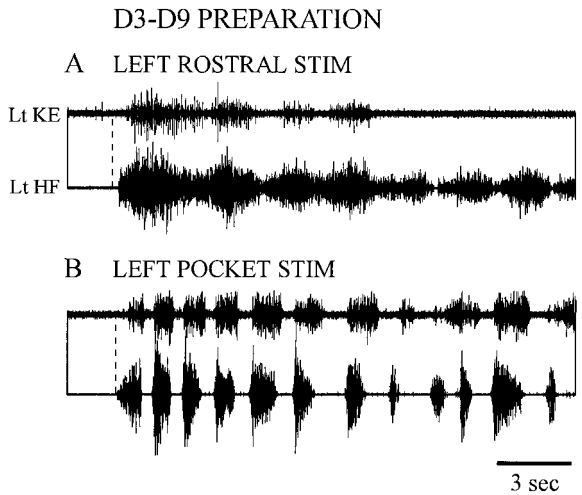

FIG. 7. Comparison of unilaterally evoked rostral and pocket scratch motor patterns in *experiment 9*, a D_3–D_9 preparation. Motor output is shown only for the left KE (AM-KE) and HF nerves. *A*; rostral scratch response to mechanical stimulation of the SP_2 site in the left rostral scratch receptive field. *B*: pocket scratch elicited by mechanical stimulation of the Fem5 site in the left pocket scratch receptive field. Vertical dashed lines indicate stimulus-onset; stimulation was continued for the remainder of each recording. Rostral scratch exhibited rhythmic HF discharge with no quiescent periods between bursts, typical of most D_3–D_9 and D_3–D_8 preparations. In contrast, the pocket scratch displayed HF bursts separated by distinct quiescent periods.

sharply defined HF bursts exhibited abrupt terminations and distinct OFF periods in every cycle. In two turtles, we had a sufficient number of pocket scratch episodes to permit a statistical comparison with rostral scratch episodes. The average percentage of cycles per episode with complete HF-OFF periods during unilateral rostral scratch and unilateral pocket scratch stimulation were as follows (average ± SD): *experiment 7*, a D_3–D_8 preparation (rostral, 10 episodes): 3.3 ± 7.0%, (pocket, 10 episodes): 91.4 ± 5.3%; *experiment 9*, a D_3–D_9 preparation (rostral, 12 episodes): 15.6 ± 18.8%, (pocket, 7 episodes): 100.0 ± 0.0%. In both experiments, the pocket scratch average was significantly higher than the rostral scratch average at $P < 0.0002$, using the Mann-Whitney *U* test (Siegel 1956). One interpretation of these data is that some interneuronal circuitry that inhibits HF is present within the D_8 and D_9 segments but is not sufficiently activated by unilateral rostral stimulation to completely terminate HF bursts. Pocket stimulation may provide stronger drive to these inhibitory elements, resulting in more complete HF burst terminations. This view also is supported by previous work that demonstrated normal pocket scratch cycles in surgically restricted spinal cord preparations (Currie and Lee 1996b; Mortin and Stein 1989).

DISCUSSION

The goal of the present experiments was to investigate mechanisms of hip rhythmogenesis during fictive rostral scratching in turtles. Our results provide evidence that reciprocal inhibition between hip circuit modules in the anterior hindlimb enlargement can generate rhythmicity during bilateral hindlimb motor patterns. We use the term ''module'' to describe the group of coactive neuronal elements that control the activity of agonist (e.g., HF) motoneurons for one limb and coordinate the activity with that of synergist and antagonist motor pools in the same limb and in the contralateral limb (Jordan 1991; Jordan et al. 1986; Stein and Smith 1997; Stein et al. 1995). We attach special significance to hip rhythm generation because previous work that examined phase-dependent resets demonstrated that hip (but not knee) motor output is linked tightly to the timing of the fictive scratch rhythm for the entire limb (Currie and Stein 1989). The importance of hip circuitry in the control of the overall limb rhythm also was demonstrated by Andersson and Grillner (1981, 1983) for fictive stepping in cats. We focus on HF activity in part because HF motoneurons (Ruigrok and Crowe 1984) and at least some HF premotor circuitry (Mortin and Stein 1989) are located in the anterior two segments of the spinal hindlimb enlargement (D_8 and D_9), while most HE circuitry is located in more posterior segments (D_{10}, S_1, S_2). The anterior segments of hindlimb enlargement are known to display the greatest rhythmogenic capacity for turtle (Mortin and Stein 1989) and cat (Deliagina et al. 1983; Gelfand et al. 1988) scratching as well as for locomotor activity in various preparations (neonatal rat: Cowley and Schmidt 1997; Kjaerulff and Kiehn 1996; cat: Grillner and Zangger 1979; chick embryo: Ho and O'Donovan 1993).

The bilateral shared core model of the turtle rostral scratch CPG proposes that HF and HE modules make reciprocal inhibitory connections with each other on the same side (e.g., right HF-HE), and with their mirror-image homologs on the opposite side (e.g., right-left HF) (Stein et al. 1995). In addition, the model suggests that HF modules make mutual crossed excitatory connections with contralateral HE modules. It is currently unknown to what extent individual HF and HE modules can be independently rhythmogenic and whether rhythmicity can be produced in the scratch network by reciprocal interactions between modules. The goal of the present experiments was to assess the capability of reciprocal inhibition between hip modules to contribute to scratch rhythmogenesis. Our approach was to transect the spinal cord at the posterior end of segment D_9 or D_8 in the anterior hindlimb enlargement, which disconnected as much HE circuitry as possible from the right and left rostral scratch networks (Figs. 1 and 8, *A1–C1*). Most of the resulting D_3–D_9 and D_3–D_8 preparations responded to unilateral stimulation of the rostral scratch receptive field with rhythmic ipsilateral HF discharge that lacked ''HF-OFF'' periods between bursts in most cycles and weak contralateral HE bursts in some preparations that were coactive with ipsilateral HF bursts (Figs. 3, *A1* and *C1*, and 8, *A1*, *A2*, *C1*, and *C2*). Thus unilateral rostral stimulation in D_3–D_9 and D_3–D_8 preparations produced activation (at the level of motoneuron discharge) of the mutually excitatory ipsilateral HF and contralateral HE modules alone, generating only weak rhythmicity. In contrast, bilateral stimulation of rostral scratch, which simultaneously excited reciprocally inhibitory hip modules on opposite sides (right and left HF) and on the same side (HF and residual HE circuitry spared by the transection), evoked vigorous alternating discharge in right and left HF nerves that exhibited enhanced HF rhythmicity on both sides (Figs. 4, 6, and 8*B*, *1* and *2*) and reconstructed HF-OFF periods between bursts (Figs. 3 and 8*B*, *1* and *2*, and Table 1). We interpret these results to mean that reciprocal inhibition between hip modules can help to terminate HF bursts and increase HF rhythmicity under conditions where mutually inhibitory modules are strongly coactivated (as during bilateral scratching). Crossed reciprocal inhibition between right and left HF modules probably contributed the most to these effects, assuming that relatively little HE circuitry remained in D_3–D_9

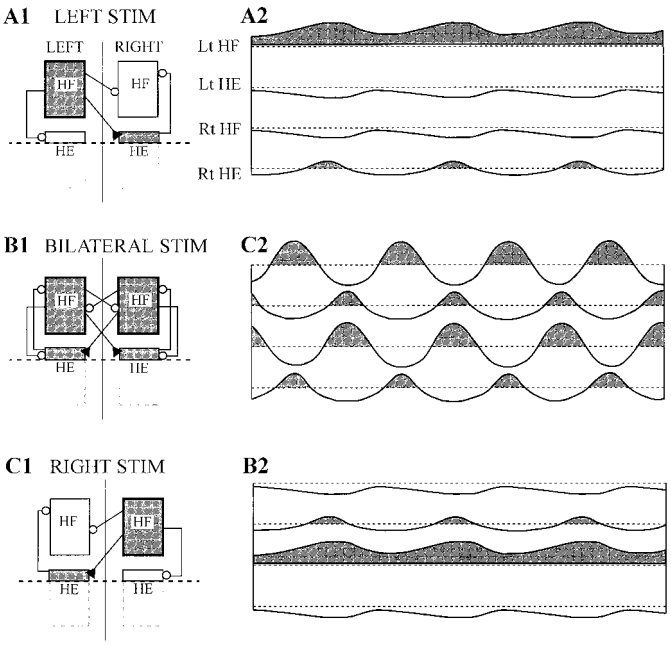

FIG. 8. Summary diagram illustrating the patterns of activity in hip circuit modules during left, bilateral, and right stimulation of rostral scratch reflex in transected (D_3–D_8 and D_3–D_9) preparations. *A1–C1*: illustration of hip circuit modules (modified from Stein et al. 1995). Shaded rectangles represent active (spiking) modules; unshaded rectangles represent inactive modules. Excitatory (filled triangles) and inhibitory (unfilled circles) synaptic outputs are shown only for active modules. Dashed lines in *A1–C1* represent spinal transections at the caudal end of the D_8 (D_3–D_8 preparations) or D_9 (D_3–D_9 preparations) segment; most HE circuitry is located caudal to the transection (light gray outlines), so is disconnected from the rostral scratch network. Some hypothetical connections within and between modules (Stein et al. 1995) were left out of these diagrams for simplicity. *A2–C2*: hypothetical voltage changes in HF and HE neurons on both sides during left, bilateral, and right stimulation of rostral scratch reflex in transected preparations. Firing threshold is shown as dotted line in *A2–C2*; shaded regions of voltage traces indicate the timing of spiking activity.

and D_3–D_8 preparations to interact with ipsilateral HF modules. Crossed inhibition also has been proposed to participate in the construction of axial locomotor rhythms in lampreys, fish, and frog embryos (reviewed in Fetcho 1991; Friesen 1994; Kiehn et al. 1997; Marder and Calabrese 1996). The relative contribution of crossed inhibition to rhythmogenesis in the turtle hindlimb enlargement can be assessed further in future experiments by observing the effects of midline spinal lesions that sever commissural pathways.

Evidence from several studies indicates that a single HF module on one side of the turtle spinal cord may be capable of some independent rhythmicity in response to rostral scratch sensory input; this is based on the observation that continuous rhythmic HF discharge (without ipsilateral HE activity) can occur spontaneously in D_3-end turtles (Robertson and Stein 1988; Robertson et al. 1985; Stein and Grossman 1980; Stein et al. 1982) or can be induced to occur with greater frequency by surgical (Mortin and Stein 1989; Stein et al. 1995, 1998; the present study) or chemical (Currie and Lee 1997) manipulations of the spinal cord. Thus these studies and the present experiments show that a single HF module can express rhythmic output without activation of the ipsilateral antagonist motoneurons. Similar independent activation of elbow flexor or extensor bursting was reported recently for the in vitro mudpuppy spinal cord (Cheng et al. 1998). In the present experiments, the turtle spinal cord was able to produce rhythmically modulated HF discharge on one side without activation of either the ipsilateral antagonist (HE) or the contralateral mirror-image (HF) motoneurons (Fig. 3, *A1* and *C1*). These observations support the view that some independent HF rhythmicity can be elicited by scratch stimuli in the absence of either crossed or uncrossed reciprocal inhibition. Experiments with in vitro mammalian spinal cords, in which inhibitory neurotransmission was blocked, also have indicated that limb rhythmogenesis can occur in the absence of synaptic inhibition (Bracci et al. 1996; Cazalets et al. 1996; Cowley and Schmidt 1995, 1997; Ho 1997; Ozaki et al. 1996). Note, however, that reciprocal inhibition between hip modules in the turtle need not necessarily produce motor output from both modules. For example, it seems plausible that a subset of ipsilateral HE and contralateral HF interneurons might be active in antiphase with the ''independent'' HF bursts on one side, without producing detectable motor output from ipsilateral HE or contralateral HF. Such ''subthreshold'' reciprocal interactions might contribute to the rhythmicity of HF motor output. Future experiments could begin to address this issue by searching with an extracellular microelectrode in the ipsilateral HE (D_{10}–S_2) and contralateral HF (D_8–D_9) areas of the spinal cord for interneuronal units that exhibit antiphasic discharge during independent HF bursting on one side.

It may be argued that bilateral stimulation of rostral scratch could increase HF rhythmicity and the occurrence of HF-OFF periods not because of reciprocal inhibitory interactions but simply because it provides more sensory drive to HF modules. A unilateral rostral stimulus, in transected D_3–D_9 and D_3–D_8 turtles, may not excite the ipsilateral HF module sufficiently for it to become rhythmically active. We believe this is unlikely for two reasons. First, one would expect that if HF modules were more intensely activated by bilateral stimulation, that this would be reflected in larger HF burst amplitudes. However, Stein et al. (1995; their Fig. 3A) showed that there was no significant difference in HF burst amplitudes during unilateral and bilateral stimulation of rostral scratch in D_3-end preparations. We also did not observe noticeably larger HF bursts during bilateral rostral stimulation in the present study (e.g., Fig. 2), although we did not quantify burst amplitudes. Second, there is no basis for believing that more intense activation of HF increases its rhythmicity and the occurrence of off periods between bursts. In fact, during a typical rostral scratch episode in D_3-end turtles, spontaneous HE-deletion cycles that lack HF-OFF periods nearly always occur at the beginning of the episode, when HF burst amplitudes are greatest (Robertson and Stein 1988; Stein et al. 1982, 1995).

Rostral and pocket scratch CPGs displayed different capacities to generate normal HF cycles in turtles where most HE circuitry was removed (D_3–D_9 and D_3–D_8 preparations). Unilateral rostral stimulation evoked rhythmically modulated discharge in ipsilateral HF motoneurons with a very low percentage of off periods between bursts (Table 1; Figs. 3 and 7*A*). In contrast, unilateral pocket stimulation elicited vigorous HF bursts separated by distinct, long-lasting off periods in nearly all cycles (Fig. 7*B*). It is unlikely that the increased occurrence of HF-OFF periods during pocket scratch was due to more intense activation of the HF module by pocket sensory input. Distinct OFF periods were present even between the weakest HF bursts in the pocket scratch (Fig. 7*B;* bursts 8 and 9) but were absent even between the strongest HF bursts in the rostral scratch (Fig. 7*A;* bursts 1 and 2). A possible explanation is that

some HE-associated interneurons (components of the ipsilateral HE module) that inhibit HF are present within the D_8 and D_9 segments and are strongly excited by unilateral pocket scratch stimulation but less excited by unilateral rostral scratch stimulation. Activation of these HE-associated inhibitory interneurons may not be sufficient during unilateral rostral stimulation to completely terminate HF bursts. Bilateral rostral stimulation may reconstruct HF-OFF periods and increase HF rhythmicity, in part, by strongly exciting these same HE interneurons (via crossed pathways) that are accessed by unilateral pocket sensory input.

We previously explored the participation of the portion of spinal cord anterior to the hindlimb enlargement (preenlargement segments D_3–D_7) in the generation of turtle rostral scratch motor rhythms (Currie and Gonsalves 1997). The D_7 spinal cord segment is immediately anterior to the hindlimb enlargement and contains two populations of motoneurons, ''TD7'' and ''OD7,'' that innervate the transverse-abdominus and oblique-abdominus respiratory muscles, respectively (Currie and Gonsalves 1997; Mortin and Stein 1989). In D_3-end turtles, unilateral stimulation of the right rostral scratch receptive field evoked rhythmic coactivation of right HF, right TD7, and left OD7 motoneurons that could alternate with weaker coactive bursts in left TD7 and right OD7. D_3–D_7 preparations had two complete spinal transections, one at D_2–D_3 and a second at D_7–D_8 that disconnected the entire hindlimb enlargement from the rostral scratch network. In D_3–D_7 turtles, unilateral stimulation of the right rostral receptive field evoked only tonic or weakly modulated discharge in right TD7 and left OD7 respiratory motoneurons. However, bilateral stimulation of rostral receptive fields reestablished vigorous bursting in which coactive right TD7 and left OD7 bursts alternated with coactive left TD7 and right OD7 bursts. These results indicated that simultaneous activation of reciprocally inhibitory circuit modules could generate rhythmicity in preenlargement networks and therefore implied that similar mechanisms might operate in the hindlimb enlargement to enhance hip rhythmicity. Furthermore because the D_7 segment exhibited little or no rhythmicity during unilateral stimulation but strong rhythmicity during bilateral stimulation, preenlargement D_7 networks may contribute significantly to the increased rhythmicity that we observed in D_3–D_9 and D_3–D_8 preparations during bilateral stimulation in the present study (Figs. 3, 4, and 6).

Pharmacological experiments support the conclusion that some but not all inhibition in turtle spinal motor networks is mediated by strychnine-sensitive glycine receptors (Currie and Lee 1996a, 1997). During the fictive flexion reflex, turtles exhibited a crossed inhibition of contralateral hip flexor activity (Currie and Lee 1996a; Currie and Stein 1989) similar to that of mammals (Eccles and Sherrington 1931; Holmqvist 1961; Jankowska et al. 1967; Sherrington 1906). The crossed inhibition associated with flexion reflex appeared to involve glycinergic transmission in turtles because it was abolished and replaced by crossed excitation after strychnine application to the hindlimb enlargement (Currie and Lee 1996a). However, during bilateral fictive rostral scratching, prolonged application of 50 μM strychnine to the turtle hindlimb enlargement produced only a slight increase in the variability of interlimb phase values (right vs. left hip flexor bursts) and did not abolish right-left (interlimb) or flexor-extensor (intralimb) alternation (Currie and Lee 1997). That result contrasts with fictive locomotion studies in which strychnine synchronized the normally alternating discharge in mirror-image right- and left-side muscle nerves (lamprey: Cohen and Harris-Warrick 1984; Hagevik and McClellan 1994; neonatal rat: Cowley and Schmidt 1995; Kremer and Lev-Tov 1997; Kudo et al. 1991; cat: Noga et al. 1993) and intralimb flexors and extensors (neonatal rat: Cowley and Schmidt 1995; cat: Kriellaars et al. 1988; Noga et al. 1995). Bilateral stimulation of rostral scratch in turtles actually reconstructed rostral scratch motor rhythms with normal interlimb (right-left HF) and intralimb (HF-HE) alternation after unilaterally evoked scratch responses were rendered almost completely tonic by strychnine (see Fig. 8 in Currie and Lee 1997). Other investigators also have described strychnine-resistant right-left alternation in fictive motor patterns elicited by chemical (Kremer and Lev-Tov 1997; McPherson et al. 1994) or electrical (Magnuson and Trinder 1997) stimulation of the spinal cord. The persistence of interlimb and intralimb alternation in the presence of strychnine implies that other transmitter systems, such as $GABA_A$ (Cowley and Schmidt 1995; Kremer and Lev-Tov 1997) and strychnine-insensitive glycine receptors (Kuhse et al. 1990) may contribute to reciprocal inhibition in turtle scratch networks. Future experiments are required to identify these transmitter systems and further assess the role of both crossed and uncrossed reciprocal inhibition in hindlimb rhythmogenesis during fictive scratching and other rhythmic motor activity, including fictive locomotion (Juranek and Currie 1998).

This research was supported by National Science Foundation Grant IBN-9723973 to S. N. Currie.

Address reprint requests to S. N. Currie.

Received 14 September 1998; accepted in final form 10 February 1999.

REFERENCES

ANDERSSON, O. AND GRILLNER, S. Peripheral control of the cat's step cycle. I. Phase dependent effects of ramp-movements of the hip during ''fictive locomotion.'' *Acta Physiol. Scand.* 113: 89–101, 1981.

ANDERSSON, O. AND GRILLNER, S. Peripheral control of the cat's step cycle. II. Entrainment of the central pattern generators for locomotion by sinusoidal hip movements during ''fictive locomotion.'' *Acta Physiol. Scand.* 118: 229–239, 1983.

BRACCI, E., BALLERINI, L., AND NISTRI, N. Spontaneous rhythmic bursts induced by pharmacological block of inhibition in lumbar motoneurons of the neonatal rat spinal cord. *J. Neurophysiol.* 75: 640–647, 1996.

CAZALETS, J. R., BORDE, M., AND CLARAC, F. The synaptic drive from the spinal locomotor network to motoneurons in the newborn rat. *J. Neurosci.* 16: 298–306, 1996.

CHENG, J., STEIN, R. B., JOVANOVIÇ, K., YOSHIDA, K., BENNETT, D. J., AND HAN, Y. Identification, localization, and modulation of neural networks for walking in the mudpuppy (*Necturus maculatus*) spinal cord. *J. Neurosci.* 18: 4295–4311, 1998.

COHEN, A. H. AND HARRIS-WARRICK, R. M. Strychnine eliminates alternating motor output during fictive locomotion in the lamprey. *Brain Res.* 293: 164–167, 1984.

COWLEY, K. C. AND SCHMIDT, B. J. Effects of inhibitory amino acid antagonists on reciprocal inhibitory interactions during rhythmic motor activity in the in vitro neonatal rat spinal cord. *J. Neurophysiol.* 74: 1109–1117, 1995.

COWLEY, K. C. AND SCHMIDT, B. J. Regional distribution of the locomotor pattern-generating network in the neonatal rat spinal cord. *J. Neurophysiol.* 77: 247–259, 1997.

CURRIE, S. N. Glutamate microinjection in the turtle spinal cord reveals the reciprocal organization of hindlimb motor networks. *Soc. Neurosci. Abstr.* 23: 207, 1997.

CURRIE, S. N. AND GONSALVES, G. G. Right-left interactions between rostral scratch networks generate rhythmicity in the preenlargement spinal cord of the turtle. *J. Neurophysiol.* 78: 3479–3483, 1997.

CURRIE, S. N. AND GONSALVES, G. G. Crossed reciprocal inhibition and scratch rhythmogenesis in the turtle spinal cord. *Ann. NY Acad. Sci.* 860: 458–460, 1998.

CURRIE, S. N. AND LEE, S. Glycinergic inhibition in the turtle spinal cord regulates the intensity and pattern of fictive flexion reflex motor output. *Neurosci. Lett.* 205: 75–78, 1996a.

CURRIE, S. N. AND LEE, S. Sensory-evoked pocket scratch motor patterns in the in vitro turtle spinal cord: reduction of excitability by an *N*-methyl-D-aspartate antagonist. *J. Neurophysiol.* 76: 81–92, 1996b.

CURRIE, S. N. AND LEE, S. Glycinergic inhibition contributes to the generation of rostral scratch motor patterns in the turtle spinal cord. *J. Neurosci.* 17: 3322–3333, 1997.

CURRIE, S. N. AND STEIN, P.S.G. Interruptions of fictive scratch motor rhythms by activation of cutaneous flexion reflex afferents in the turtle. *J. Neurosci.* 9: 488–496, 1989.

CURRIE, S. N. AND STEIN, P.S.G. Cutaneous stimulation evokes long-lasting excitation of spinal interneurons in the turtle. *J. Neurophysiol.* 64: 1134–1148, 1990.

DELIAGINA, T. G., ORLOVSKY, G. N., AND PAVLOVA, G. A. The capacity for generation of rhythmic oscillations is distributed in the lumbosacral spinal cord of the cat. *Exp. Brain Res.* 53: 81–90, 1983.

ECCLES, J. C. AND SHERRINGTON, C. S. Studies on the flexor reflex. VI. Inhibition. *Proc. R. Soc. Lond. B Biol. Sci.* 109: 91–113, 1931.

FETCHO, J. R. Spinal network of the Mauthner cell. *Brain Behav. Evol.* 37: 298–316, 1991.

FRIESEN, W. O. Reciprocal inhibition: a mechanism underlying oscillatory animal movements. *Neurosci. Biobehav. Rev.* 18: 547–553, 1994.

GELFAND, I. M., ORLOVSKY, G. N., AND SHIK, M. L. Locomotion and scratching in tetrapods. In: *Neural Control of Rhythmic Movements in Vertebrates*, edited by A. H. Cohen, S. Rossignol, and S. Grillner. New York: Wiley, 1988, p. 285–332.

GRILLNER, S. AND ZANGGER, P. On the central generation of locomotion in the low spinal cat. *Exp. Brain Res.* 34: 241–261, 1979.

HAGEVIK, A. AND MCCLELLAN, A. D. Coupling of spinal locomotor networks in larval lamprey revealed by receptor blockers for inhibitory amino acids: neurophysiology and computer modeling. *J. Neurophysiol.* 72: 1810–1829, 1994.

HO, S. M. Rhythmic motor activity and interlimb co-ordination in the developing pouch young of a wallaby (*Macropus eugenii*). *J. Physiol. (Lond.)* 501: 623–636, 1997.

HO, S. M. AND O'DONOVAN, M. J. Regionalization and intersegmental coordination of rhythm-generating networks in the spinal cord of the chick embryo. *J. Neurosci.* 13: 1354–1371, 1993.

HOLMQVIST, B. Crossed spinal reflex actions evoked by volleys in somatic afferents. *Acta Physiol. Scand. Suppl. 181* 52: 1–66, 1961.

JANKOWSKA, E., JUKES, M.G.M., LUND, S., AND LUNDBERG, A. The effect of DOPA on the spinal cord. 5. Reciprocal organization of pathways transmitting excitatory action to alpha motoneurones of flexors and extensors. *Acta Physiol. Scand.* 70: 369–388, 1967.

JORDAN, L. M. Brainstem and spinal cord mechanisms for the initiation of locomotion. In: *Neurobiological Basis of Human Locomotion*, edited by M. Shimamura, S. Grillner, and V. R. Edgerton. Tokyo: Japan Scientific Societies Press, 1991, p. 3–20.

JORDAN, L. M., BROWNSTONE, R. M., KRIELLAARS, D. J., AND NOGA, B. R. Spinal modules for walking movements revealed in fictive locomotion experiments. *Soc. Neurosci. Abstr.* 12: 877, 1986.

JURANEK, J. AND CURRIE, S. N. Fictive swimming elicited by electrical stimulation of the turtle spinal cord: interactions with scratch reflex. *Soc. Neurosci. Abstr.* 24: 1669, 1998.

KIEHN, O., HOUNSGAARD, J., AND SILLAR, K. T. Basic building blocks of vertebrate spinal central pattern generators. In: *Neurons, Networks, and Motor Behavior*, edited by P.S.G. Stein, S. Grillner, A. I. Selverston, and D. G. Stuart. Cambridge: MIT Press, 1997, p. 47–59.

KJAERULFF, O. AND KIEHN, O. Distribution of networks generating and coordinating locomotor activity in the neonatal rat spinal cord in vitro: a lesion study. *J. Neurosci.* 16: 5777–5794, 1996.

KREMER, E. AND LEV-TOV, A. Localization of the spinal network associated with generation of hindlimb locomotion in the neonatal rat and organization of its tranverse coupling system. *J. Neurophysiol.* 77: 1155–1170, 1997.

KRIELLAARS, D. J., FORTIER, P., AND JORDAN, L. M. Strychnine-sensitive components of the spinal modules for hindlimb locomotion in the cat. *Soc. Neurosci. Abstr.* 14: 264, 1988.

KUDO, N., OZAKI, S., AND YAMADA, T. Ontogeny of rhythmic activity in the spinal cord of the rat. In: *Neurological Basis of Human Locomotion*, edited by M. Shumamura, S. Grillner, and V. R. Edgerton. Tokyo: Japanese Scientific Society, 1991, p. 127–136.

KUHSE, J., SCHMIEDEN, V., AND BETZ, H. A single amino acid exchange alters the pharmacology of neonatal rat glycine receptor subunit. *Neuron* 5: 867–873, 1990.

LENNARD, P. R. AND STEIN, P.S.G. Swimming movements elicited by electrical stimulation of the turtle spinal cord. I. Low-spinal and intact preparations. *J. Neurophysiol.* 40: 768–778, 1977.

MAGNUSON, D.S.K. AND TRINDER, T. C. Locomotor rhythm evoked by ventrolateral funiculus stimulation in the neonatal rat spinal cord in vitro. *J. Neurophysiol.* 77: 200–206, 1997.

MARDER, E. AND CALABRESE, R. L. Principles of rhythmic motor pattern generation. *Physiol. Rev.* 76: 687–717, 1996.

MCPHERSON, D. R., BUCHANAN, J. T., AND KASICKI, S. Effects of strychnine on fictive swimming in the lamprey: evidence for glycinergic inhibition, discrepancies with model predictions, and novel modulatory rhythms. *J. Comp. Physiol. [A]* 175: 311–321, 1994.

MORTIN, L. M., KEIFER, J., AND STEIN, P.S.G. Three forms of the scratch reflex in the spinal turtle: movement analyses. *J. Neurophysiol.* 53: 1501–1516, 1985.

MORTIN, L. I. AND STEIN, P.S.G. Spinal cord segments containing key elements of the central pattern generators for three forms of scratch reflex in the turtle. *J. Neurosci.* 9: 2285–2296, 1989.

MORTIN, L. I. AND STEIN, P.S.G. Cutaneous dermatomes for initiation of three forms of the scratch reflex in the spinal turtle. *J. Comp. Neurol.* 295: 515–529, 1990.

NOGA, B. R., COWLEY, K. C., HUANG, A., JORDAN, L. M., AND SCHMIDT, B. J. Effects of inhibitory amino acid antagonists on locomotor rhythm in the decerebrate cat. *Soc. Neurosci. Abstr.* 19: 540, 1993.

OZAKI, S., YAMADA, T., IIZUKA, M., NISHIMARU, H., AND KUDO, N. Development of locomotor activity induced by NMDA receptor activation in the lumbar spinal cord of the rat fetus studied in vitro. *Dev. Brain Res.* 97: 118–125, 1996.

ROBERTSON, G. A., MORTIN, L. I., KEIFER, J., AND STEIN, P.S.G. Three forms of the scratch reflex in the spinal turtle: central generation of motor patterns. *J. Neurophysiol.* 53: 1517–1534, 1985.

ROBERTSON, G. A. AND STEIN, P.S.G. Synaptic control of hindlimb motoneurones during three forms of the fictive scratch reflex in the turtle. *J. Physiol. (Lond.)* 404: 101–128, 1988.

RUIGROK, T.J.H. AND CROWE, A. The organization of motor neurons in the turtle lumbar spinal cord. *J. Comp. Neurol.* 228: 24–37, 1984.

SHERRINGTON, C. S. *The Integrative Action of the Nervous System.* New Haven, CT: Yale Univ. Press, 1906.

SIEGEL, S. *Nonparametric Statistics for the Behavioral Sciences.* New York: McGraw-Hill, 1956.

STEIN, P.S.G. AND GROSSMAN, M. L. Central program for scratch reflex in turtles. *J. Comp. Physiol. [A]* 140: 287–294, 1980.

STEIN, P.S.G., MCCULLOUGH, M. L., AND CURRIE, S. N. Reconstruction of flexor/extensor alternation during fictive rostral scratching by two-site stimulation in the spinal turtle with a transverse spinal hemisection. *J. Neurosci.* 18: 467–479, 1998.

STEIN, P.S.G., ROBERTSON, G. A., KEIFER, J., GROSSMAN, M. L., BERENBEIM, J. A., AND LENNARD, P. R. Motor neuron synaptic potentials during fictive scratch reflex in turtle. *J. Comp. Physiol. [A]* 146: 401–409, 1982.

STEIN, P.S.G. AND SMITH, J. L. Neural and biomechanical control strategies for different forms of vertebrate hindlimb motor tasks. In: *Neurons, Networks and Motor Behavior*, edited by P.S.G. Stein, S. Grillner, A. I. Selverston, and D. G. Stuart. Cambridge, MA: MIT, 1997, p. 61–73.

STEIN, P.S.G., VICTOR, J. C., FIELD, E. C., AND CURRIE, S. N. Bilateral control of hindlimb scratching in the spinal turtle: contralateral spinal circuitry contributes to the normal ipsilateral motor pattern of fictive rostral scratching. *J. Neurosci.* 15: 4343–4355, 1995.

ZANGERL, R. The turtle shell. In: *Biology of the Reptilia*, edited by C. Gans. New York: Academic, 1969, vol. 1, p. 311–339.